JOURNAL OF MATERIALS SCIENCE **35** (2000) 5207–5213

Mechanical properties of the double gyroid phase in oriented thermoplastic elastomers

B. J. DAIR
Department of Materials Science and Engineering, Massachusetts Institute of Technology, Cambridge, MA 02139, USA

A. AVGEROPOULOS, N. HADJICHRISTIDIS
Department of Chemistry, University of Athens, Panepistimiopolis, 157 71 Zougrafou, Athens, Greece

E. L. THOMAS*
Department of Materials Science and Engineering, Massachusetts Institute of Technology, Cambridge, MA 02139, USA
E-mail: elt@mit.edu

We investigate the mechanical properties of triblock copolymers with oriented double gyroid (DG) morphology in poly(styrene-b-isoprene-b-styrene) (SIS) triblock copolymers by deforming textured samples along both the [111] direction and transverse to this direction. The modulus anisotropy for the two directions of this cubic material is approximately a factor of 5. Deformation along [111] causes the sample to form a distinct neck and draw, while the deformation in the transverse direction proceeds without neck formation. In addition, the mechanical hysteresis of the [111] stretch is 50% higher than that transverse to the [111] direction. Upon unloading and annealing above the polystyrene Tg, the DG structure recovers fully, both macroscopically and microscopically. The mechanical properties of the DG are compared to those of the classical block copolymer morphologies to gain insight into the deformation mechanism.

1. Introduction

In a previous paper [1], we presented the first work on the mechanical properties and deformation behavior of the double gyroid (DG) morphology in block copolymers. It was shown that the unoriented polygranular DG elastomeric films exhibit stress-strain behavior with superior yield stress and toughness to the spherical, cylindrical, and lamellar microdomain morphologies. Remarkably, the DG was the only polygranular unoriented polyisoprene (PI)-rich morphology which exhibited necking and drawing phenomena. However, because grains in the polygranular sample have different orientations with respect to the stretching axis, the deformation behavior of an isotropic sample is a superposition of the responses of different orientations to the applied stress. Indeed, the cubic symmetry of the double gyroid confers inherent mechanical anisotropy. Therefore well-oriented samples are necessary to explore the mechanical anisotropy and to elucidate the mechanisms of deformation.

Keller and associates at the University of Bristol were pioneers of orienting and studying the deformation behavior of block copolymers, mainly with the glassy polystyrene (PS) cylinder morphology, globally oriented via extrusion [2–4]. Odell and Keller [5] used SAXS, TEM, and birefringence to study the anisotropy and the deformation behavior of oriented cylinders both parallel and perpendicular to the cylinder axes. Arridge and Folkes used Keller's samples to study the small strain mechanical anisotropy and made comparison to composite mechanics [6]. By employing roll casting and annealing we have globally oriented DG films of an elastomeric poly(styrene-b-isoprene-b-styrene) (SIS) triblock copolymer system. Upon roll casting the SIS triblock the morphology is highly textured cylinders, aligned along the roll cast direction. Upon annealing, the DG phase nucleates and grows epitaxially with the [111] direction oriented along the cylinder axes [7]. In this paper we present the mechanical properties of textured films with the double gyroid microdomain structure and discuss the observed stress-strain behavior with respect to fundamental block copolymer concepts.

2. Experimental

An equilibrium tricontinuous cubic morphology forms by simple solvent casting and annealing of a neat 34 vol% (37 wt%) polystyrene SIS triblock copolymer with block molecular weights: 13.6K-46.4K-13.6K, and PDI = 1.04 [8]. This same polymer was oriented via roll casting, a process shown to macroscopically orient block copolymer films of cylinders and lamellae. The roll casting technique is described in papers by

* Author to whom all correspondence should be addressed.

Albalak *et al.* [9, 10], and the processing parameters as well as the morphological characterization of the resulting textured DG films are reported in a previous paper [7]. Tensile samples 1–2 mm wide × 15–20 mm long were cut from 0.6–1.0 mm—thick films either along or perpendicular to the roll cast direction. An Instron 4501 equipped with a 10 N or 5 kN load cell was used to gather the tensile data. The software Instron Series IX was run on a PC which was interfaced to the 4500 Instron controller. Samples 9–15 mm in gauge length were stretched to 600% and then unloaded at a constant crosshead velocity of 2.6 mm/min.

3. Results and discussion

3.1. Mechanical properties of the DG

Double gyroid films produced via roll casting orient with the [111] along the flow direction [7]. For cubic materials, central sections of the Young's Modulus surface normal to ⟨111⟩ are circles [11]; that is, Young's modulus is isotropic within a plane transverse to the [111] direction. Properties in directions transverse to the [111] axis for large strain, e.g. yielding and beyond, may depend on the particular direction of stretch. However, because the ⟨110⟩ and ⟨112⟩ directions alternate around the [111] axis every 30°, a mosaicity of only ±15° will create apparent isotropy in these properties as well. The modulus, large strain properties, and deformation mechanisms for loads applied in a direction normal to the [111] axis will thus be referred to as "transverse."

Fig. 1 shows representative stress-strain curves of oriented DG stretched in the [111] and transverse directions, along with the deformation response of isotropic DG. Table Ia shows the relevant tensile properties upon stretching, and Table Ib shows some relevant properties upon unloading from 600% strain.

The tensile modulus along the [111] direction was found to be approximately 50 MPa, while the modulus along the transverse direction was found to be approximately 10 MPa, rendering the anisotropy factor, or the ratio of the moduli in two different directions, $E_{\parallel}/E_{\perp} =$ 5. This relatively large anisotropy is unusual; most cubic metals have an anisotropy typically between 1 and 3 [12].

When DG is deformed along the [111] direction, yield occurs at approximately 15% strain and approximately 3.4 MPa, accompanied by formation of a distinct, visible neck,† a load drop in the force-elongation curve, and neck propagation at constant stress. Necking also occurs in isotropic polygranular films of DG [1] and also in oriented samples of the cylinder and lamellar morphologies when stretching parallel to the axes of cylinders [5, 15–18] and parallel to the layers of lamellae [19]. The hysteresis (which is an indication of the relative elastic vs. plastic or viscoelastic processes which are activated during deformation) in the DG stress-strain curve is approximately 65%, higher than that of the isotropic sample, and a strong Mullins

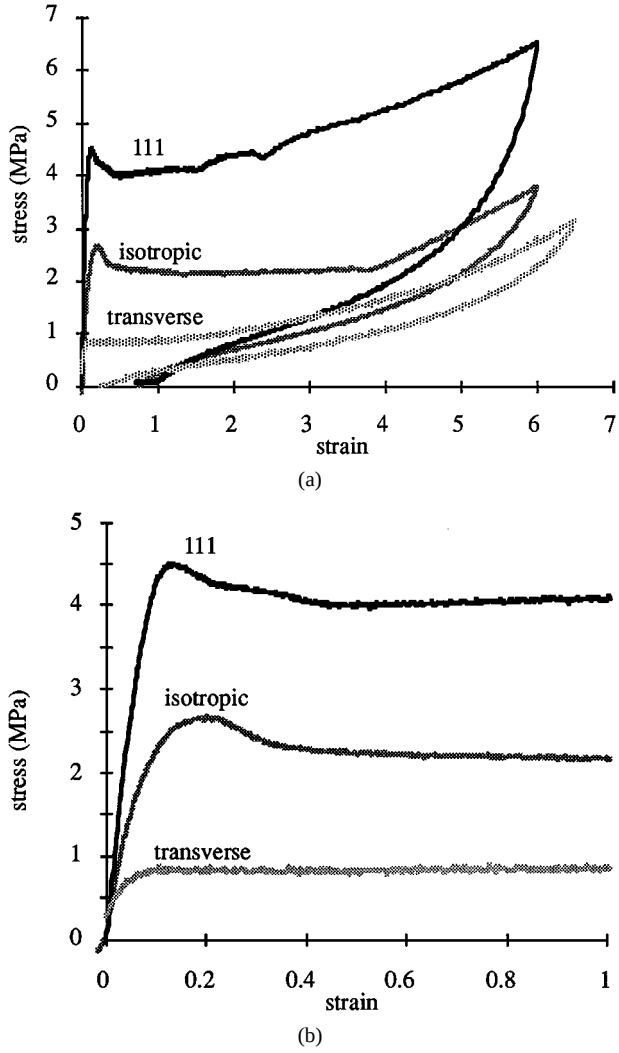

Figure 1 (a) Overlayed stress-strain curves of oriented DG stretched in the [111] and transverse directions, as well as a stress-strain curve for polygranular isotropic DG, deformed to 600% strain. (b) Enlarged view of the stress-strain curves for 0–100% strain.

effect (which is another indication of the relative elastic vs. plastic or viscoelastic processes) is observed. These features suggest a slow recovery of the deformed PS domains and microdomain grains and/or that the PS networks break when stretched beyond the yield point.

When DG is deformed along the transverse direction, yield occurs without the presence of necking. This phenomenon is also observed in stretching perpendicular to the axes of cylinders [5, 20] and perpendicular to the layers of lamellae [19]. The hysteresis in the stress-strain curve is approximately 40% and a weak Mullins effect is observed. Both these effects suggest that the rubber is carrying more of the deformation at high strains, since the deformation behavior in this direction is more akin to that of a gum vulcanizate, whereas in the [111] direction the deformation behavior was much more "plastic."

As shown by Fig. 1 and Table Ia and b, the stress-strain curve and mechanical properties of the isotropic stretch are everywhere intermediate between those of the [111] and transverse stretches, indicating that the [111] direction may be the one most resistant to deformation and the transverse direction one of the easiest directions of deformation for this structure. In

† Necking behavior is defined as "a maximum load followed by non-uniform deformation" [13, 14] and a discrete neck may be observed as a region of decreased cross-sectional area in a localized length of the sample.

comparison to the two other block copolymer morphologies with continuous domains, the DG has an anisotropy closer to lamellae than to cylinders. The factor of anisotropy between stretching parallel and perpendicular to the cylinder axis is approximately 100 [5, 20], while that of lamellae is found to be 3 [19].

In the materials studied here, the samples both microscopically and macroscopically return to their original states upon annealing for 5 days at 120° C. The SAXS patterns after annealing are almost identical to the pattern at start; long range order was restored (as seen by the number of higher order harmonics) and all original Bragg peaks returned to the same q's [21, 22]. In addition, samples return to their original dimensions when annealed, indicating full macroscopic recovery.

3.2. Geometry of the PS networks

Understanding the mechanical response of this interpenetrating nanocomposite can be done with attention to the stiff, strong glassy networks which dominate over the soft elastomeric component and control the initial tensile modulus and the flow stress of the material. The geometry of the DG microdomain structure along the [111] and transverse to the [111] is described here in order to better understand the effects on the anisotropy of mechanical behavior and properties. The DG structure of the SIS triblock consists of PS struts, or connectors, leading from one tri-functional node to another. Examination of the skeletal graph [23, 24] of the double gyroid structure shows that the axes of the PS struts are everywhere oriented along ⟨110⟩ type directions.

A cross-sectional area normal to the [111] direction (i.e., the (111) plane) of the DG is shown in Fig. 2a. The area outlined by the hexagon is the base of the cell in this plane, such that a prism built on such a base would encompass the same volume as that of the conventional cubic unit cell defined by the usual set of six {100}-type planes. The DG structure contains two 3-fold screw axes and one 3-fold inversion axis per translational unit in the (111) plane. As can be seen from Fig. 2b, PS domains surrounding the 3_1 and 3_2 screw axes reinforce the DG in the [111] direction, but the PS domains are not continuous along the $\bar{3}$ axes.

TABLE Ia Mechanical properties of the double gyroid (values averaged over 5 samples)

Stretch direction	Initial modulus (MPa)	Necking behavior?	Yield stress (MPa)	Yield strain
Isotropic	29 ± 5	Yes	2.6 ± 0.5	0.20 ± 0.02
[111]	48 ± 9	Yes	3.4 ± 0.7	0.15 ± 0.04
Transverse	9.6 ± 3.2	No	0.74 ± 0.09	0.09 ± 0.03

Six struts span the DG prism shown in Fig. 2b in the [111] direction over a distance of $\sqrt{3}a$ (where a is the DG lattice parameter.) The total volume of the prism is a^3, i.e., the same as that of a unit cube. The 3_1 and 3_2 screw axes alternate around the corners of the prism. Along [111], the struts form tight helices (likened to a stretched-out spring), each strut angled at 35° from the [111] axis. The $\bar{3}$ axis runs through the center of the prism and intersects 4 nodes (of alternating networks) stacked in the [111]. The PS struts emanating from these nodes are not connected along the [111] direction.

Along the [111] direction the PS strut segments provide reinforcement with $\sqrt{3}$ of these helical PS paths per a^2. Along the various transverse directions the most direct continuous PS paths are much more serpentine than in the [111] direction. This can be understood from examination of continuous PS paths along the ⟨112⟩ and ⟨110⟩ directions. The shortest path from one point to an identical one in a {111} plane along a ⟨110⟩-type direction is 6 struts, as shown in Fig. 2c–d, spanning a projected distance of $a\sqrt{2}$, and the shortest path along a ⟨112⟩-type direction is 10 struts, as shown in Fig. 2e–f, spanning a projected distance of $a\sqrt{6}$.

The approximate shape of a PS strut in the elastomeric triblock with DG microdomain morphology studied here with 34 vol% PS networks is shown in Fig. 3, as was determined through level-set modelling of the intermaterial dividing surfaces [25]. In our copolymer, the length of each strut is approximately 22 nm with the minimum strut diameter approximately 7 nm. (In comparison, commercially available elastomeric triblocks with PS cylindrical microdomain morphology and total molecular weight of about 100 kg/mol have cylinder diameters of about 16 nm [20] while those with a lamellar morphology and total molecular weight of about 80 kg/mol have PS layer thicknesses of about 14 nm [26].)

The small strain deformation response will depend primarily on the 3D PS networks. Depending on the loading direction, the variously oriented connected PS struts in the network will experience different types of loading from the applied load and the Poisson contraction-induced lateral forces of the rubbery matrix. Although tensile loading in the [111] direction puts the [111] 3_1 and 3_2 PS helices in tension, the PS helices along the [111], [111], and [11$\bar{1}$] directions (which are at 109° 28′ from the loading axis) are placed into compression and shear.

Loading along [111] exhibits the highest modulus, likely because this direction has the greatest continuously connected PS content per area. Loading in the directions transverse to the [111] do not result in the load direction coinciding with tightly connected set of

TABLE Ib Mechanical properties of the double gyroid after stretching to 600% strain (values averaged over 5 samples)

Stretch direction	Residual strain	Hysteresis	Mullins effect	Microscopic recovery?[a]	Macroscopic recovery?[a]
Isotropic	0.74 ± 0.06	0.50 ± 0.03	Medium	Full	Full
[111]	0.93 ± 0.04	0.66 ± 0.02	Strong	Full	Full
Transverse	0.18 ± 0.08	0.41 ± 0.04	Low	Full	Full

[a]After annealing for 5 days at 120° C.

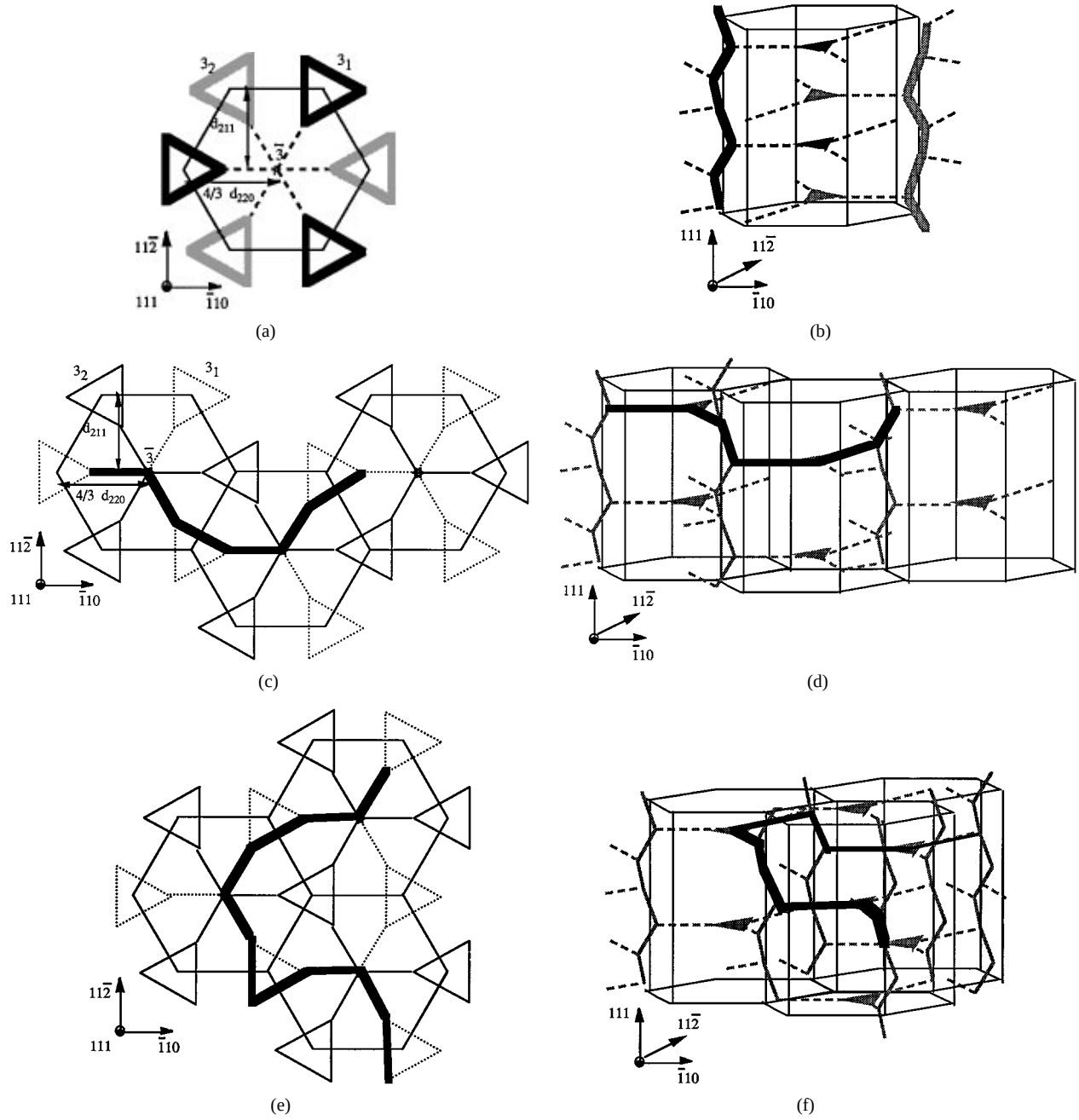

Figure 2 (a) Cross-sectional area view of the DG down the [111] direction. The black and grey lines denote the two distinct networks, and the bolded lines indicate the helical paths in the [111] direction. (b) Perspective view of the prism of the DG phase with the hexagonal base shown in Fig. 2a. The bolded lines indicate struts which contribute to the [111] modulus, and the dashed lines indicate struts which do not. The area of the base is $4\, d_{\bar{2}20}\, d_{11\bar{2}}$. (c) Sample [110] helix, whose path is outlined by the bolded lines, in the cross-sectional area view of the DG down the [111] direction. The solid and dashed lines indicate the two distinct networks. (d) Perspective view of the [110] helix shown in Fig. 2c. (e) Sample [112] helix, whose path is outlined by the bolded lines, in the cross-sectional area view of the DG down the [111] direction. (f) Perspective view of the [112] helix shown in Fig. 2e.

PS struts. Rather, the connected PS pathways are loaded primarily in shear and compression, resulting in a lower material stiffness. In both types of loading, the strut geometry lends itself to localized necking in tension due to the constricted shape and to localized buckling in compression due to the hinge-like node junctions of the PS network.

3.3. Deformation behavior of the DG

In the following sections, the mechanical properties and behavior of the DG morphology in elastomeric glassy-rubbery triblock systems will be discussed with respect to past work on the deformation behavior of polydiene (PD)-rich poly(styrene-b-diene-b-styrene) (SDS) block copolymers with cylindrical and lamellar morphologies.

3.3.1. Yielding and plastic deformation

In polymeric materials, plastic deformation, or that deformation which is not recovered upon immediate unloading, may occur by such mechanisms as necking, crazing, shear-banding, brittle failure, and/or molecular re-orientation of chains. A magnified portion of the stress-strain curves at low strains (Fig. 1b) shows that the sample stretched in the transverse direction undergoes distributed yield. A sharp yield, such as exhibited by necking or perfect elastic-plastic behavior, is indicative that all elements within a volume or subvolume

Figure 3 Schematics of skeletal graph (dark) and the intermaterial dividing surface of DG having overall 34% volume fraction PS. Shown here are two nodes connected by a strut, whose shape is constricted in the middle. Nanonecks may initiate in the thin centers of each PS strut. Picture courtesy of Jim Hoffman.

yield simultaneously, whereas a distributed yield is indicative that there are highly variable stress concentrations in the sample, for example, due to different orientations and/or grain structures.

Some early studies of the plastic deformation of compression-molded cylinder and lamellar block copolymer morphologies suggest the "break-up" of continuous PS into discrete domains [5, 17, 26, 27]. In contrast, Smith and Dickie [29] and Smith [30] postulated that plastic deformation in these materials relates to the stretching of the hard material beyond yield and is due to the ductility of the continuous PS domains. Both situations of breakage and yielding/drawing of the glassy material may occur to some degree in the cylinder and lamellar morphologies, and the size of the PS domains (i.e. PS molecular weight), the geometry of the microdomain morphology, as well as the direction of the force relative to the axes of the PS domains may all be factors in determining which mechanism dominates.

Bulk PS with molecular weight greater than the PS entanglement molecular weight ($M_e = 35$ kg/mol) crazes when stretched in tension. A PS craze contains about 50% oriented or elongated polymer "fibrils" and 50% void volume [31–33, 34]. These fibrils are cylindrical in shape and contain highly elongated chains. The natural draw ratio of PS craze fibrils in air is about $\lambda = 4$ [35, 36], and the diameter of a fibril is about 4–10 nm, with an average value of 6 nm [37–39]. The struts of the DG nanocomposites studied here, having diameters of $\sim$7 nm, are on the length scale of a craze fibril such that normal crazing or shear banding mechanisms of the bulk PS cannot occur. Rather, the PS struts themselves, which are surrounded with rubbery PI, may be more viscoelastic-plastic in character and undergo orientation as in PS craze fibrils. Cylinders and lamellae, with typical PS domain thickness somewhat larger than for our triblock, are also uniform in size throughout, and therefore may be more prone to deformation via break-up of the PS domains when stretched in the direction parallel to the continuous domains. Plasticity and viscoelasticity may therefore play more of a role in the deformation process in the DG than in either cylinders or lamellae.

The molecular weight of the end PS blocks (14 kg/mol) is much less than the entanglement molecular weight of PS (35 kg/mol). At high strains, pullout of the PS chains may therefore occur, especially if the behavior of the PS domains is viscoelastic. Under certain conditions, some struts may draw down to become separate pieces.

The loading direction relative to the PS domains will affect the forces felt by the PS domains. Let us first consider loading in the direction of highest PS continuity. The complex geometry of the DG morphology will affect the forces felt by the individual struts and nodes. Because of the 3-dimensionality of the PS networks, loading in the [111] direction will place different struts and nodes into different states of bending, tension, and shear. Struts themselves have an initial constricted shape (as shown in Fig. 3), which, when placed in tension along their axes, may begin to 'nano'-neck in the centers where the diameter is smallest, possibly followed by drawing of the PS. Under shear or bending the struts may also tend to rotate about the centers of the nodes in a similar manner as a hinge.

When cylinders and lamellae are stretched in their transverse directions, Poisson compression causes the PS cylinders (which are a 1-dimensionally-constrained system in compression) to deform by bending into "chevrons" [18] and lamellae (which are a 2-dimensionally-constrained system) to deform by buckling or "kinking" [19, 40, 41]. DG is a 3-dimensionally-constrained system due to the 3-dimensionality of the PS network connectivity so that the loading is more uniformly shared by the variously oriented PS domains.

3.3.2. Necking phenomenon

There are two phenomena which can produce load drops in tension. If the strain hardening rate is low in tension and the plastic resistance (yield stress) is high, then the load will drop upon yielding. This phenomenon is associated with loading in tension only, and as such, would be eliminated by loading in compression. The other phenomenon is associated with yielding of an aged glassy polymer and occurs regardless of testing geometry. An initially high force is necessary to either create the additional critical amount of "free volume" for molecular mobility to initiate plastic flow. Since the DG samples were well-annealed/aged above Tg before being tested and since PS domains are loaded both in tension and compression no matter what the loading direction, the two responses will be overlapped without distinction.

3.3.3. Strain hardening

Strain hardening in polymers can arise from an increase in the stiffness along the stress direction as the domains of the material re-orient toward the stress axis and/or

due to increased molecular orientation including strain-induced crystallization. In a crosslinked atactic noncrystalline rubber, strain hardening arises from molecular extension of the chains. In a crosslinked crystallizable rubber, strain hardening arises from molecular extension and strain-induced crystallization. In a glassy- or crystalline-block reinforced material, strain hardening arises from rotation or alignment of stiff units into the force direction.

Strain-induced crystallization requires stereoregularity along with molecular mobility for the reorganization of the chains. Upon elongation, either *cis*- or *trans*-isoprene units can crystallize if they occur in sufficient block lengths. However, the anionically polymerized PI in these DG samples has a mixed chain microstructure (70% cis, 20% trans, 10% 3, 4 and 1, 2) [8], but there the random sequence of isomers prohibits crystallization upon elongation. Thus, in these samples, strain hardening is due to the orientation of both the PS domains and the PI chains. One or more localized necks form somewhere along the gauge length. The material in the neck elongates to the composite's natural draw ratio, and a further increase in the strain of the strain-hardened material (beyond the natural draw ratio) requires a much higher stress than is present in the necked material. As the strain is increased further, PS domains and PI chains on the shoulder of the neck become aligned at the same macroscopic level of stress and are drawn into the neck. The cold drawing phenomenon is exhibited in the stress-strain curve by a plateau region (after the load-drop due to neck formation), which terminates at a strain indicative of the natural draw ratio of the material.

Once the neck has propagated far enough to engulf the entire gauge length to the natural draw ratio $\lambda \approx 3.75$, further deformation is possible only by either pulling out or breaking entanglements in the PI phase, or by further molecular orientation in either (or both) of the PS or PI domains. All of these mechanisms require increasingly higher and higher stress, which exhibits itself as an upturn in the stress-strain curve beyond the plateau region.

3.3.4. Viscoelastic vs. irreversible deformation processes

As with the cylindrical and lamellar microdomain morphologies, Mullin's (or the stress softening) effect, hysteresis, and residual strain after unloading are observed. Early researchers of these effects attributed them to the breakage of continuous PS domains [40, 42–44], but other factors, such as voiding, flow, and viscoelasticity of the PS domains, were not considered. Voiding and flow create permanent, irreversible deformation, while viscoelasticity does not. In vertically stretched samples, horizontal streaks through the center of SAXS patterns would indicate voiding. These do not occur in samples which are wider than the beam at all strains.[‡]

[‡] In stretches where the sample width becomes smaller than the X-ray beam diameter at the highest strains, streaking occurred through the center due to scattering off the edge of the sample. Streaks through the center do not occur in samples which are wider than the beam at all strains.

In some instances, what appears to be permanent deformation is a consequence of anelasticity or of long-time-scale viscoelasticity, but is not irrecoverable. As was previously mentioned, deformation not recovered upon immediate unloading was found to be recoverable at long times or high temperatures. This complete memory and recovery of the samples implies long-time-scale viscoelasticity. Any pullout of the chains in the plastically deformed PS domains, which are not entangled ($M < M_e$), can diffuse back to an equivalent state such that the PS domains recover their equilibrium dimensions and spacings. It can then be inferred that the entangled PI chains provide a retractive force and memory for unloading, a mechanism first postulated by Smith [30]. The increase in PS/PI interfacial area and decrease in PS strut cross-sectional area (which induces PS chain conformational changes as well as changes in location and number per area of junctions) provide yet another type of memory. Due to such internal stresses in both the PS and PI domains, a stretched and then unloaded specimen can recover its original dimensions and initial domain configuration even if some PS domains were ruptured during the deformation.

The viscoelastic properties also explain the Mullin's effect and hysteresis. The end-anchored and entangled PI chains provide the retractive force and memory during unloading, but as was mentioned by Smith and Dickie [29], the residual strain of the slow-recovering PS domains keep the rubber in tension. This causes a lowering of the stresses for a given deformation upon the second stretch, which appears as a Mullin's effect and hysteresis. This complete recovery is a special property of these styrene-diene-styrene elastomeric triblock copolymers. It was even noticed in the early studies of commercial elastomeric triblocks that upon annealing the samples recover their original dimensions [29, 42]. Although the times scales for complete recovery are long, they can be accelerated with temperature.

The Mullin's effect, hysteresis, and residual strain are more pronounced at higher styrene contents in cylinders and lamellae [1]. The magnitudes of these effects are related to the continuity of the PS domains in a given direction and of the amount of work done during the initial stretch that was not recovered immediately upon unloading. Taking all these observations together, plasticity and viscoelasticity may play a significant role in the deformation processes in the DG morphology than in either the cylindrical or lamellar microdomain morphologies.

4. Conclusions

The mechanical anisotropy of the double gyroid phase was studied using oriented samples placed in uniaxial tension parallel and transverse to the [111]. It was found that the Young's modulus is 5 times higher in the [111] direction than in the transverse direction. A distinct neck forms and propagates at a constant drawing stress for stretching parallel to the [111] direction. Stretching transverse to the [111] gives diffuse yielding without a distinct neck. The [111] direction shows high levels of hysteresis, residual strain and Mullins effects, while the direction transverse to the [111] exhibits low

values of these properties. The [111] direction is likely the most resistant to deformation and the transverse direction one of the easiest directions of deformation for this structure. This may be attributable to the presence of tight PS helical paths along [111], whereas there are no direct continuous PS path transverse to the [111]. The stress-strain curve of an isotropic polygranular DG sample is intermediate between the [111] parallel and transverse stretches of an oriented sample, indicating that properties of the DG are not as strongly dependent on the direction of stretch as in the cylinder morphology [5, 20].

A primary mechanism of deformation in the DG microdomain morphology may be yielding and plastic flow of the PS struts when these are subjected to tension. Nanonecking of the struts is a possibility, considering the constricted shape. The other micromechanism of deformation is likely to be buckling of the continuous PS domains for loading in shear and compression at the nodes in the PS networks.

Acknowledgements

We would like to thank Professors Yachin Cohen, Ali Argon and Mary Boyce for scientific discussion and Dr. Christian Honeker for construction of the stretching apparatus. This research was supported by the Air Force (AFOSR F49620-97-1-0385) and by the National Science Foundation (NSF DMR 98-07591). Fig. 3 was produced by J. Hoffman using TEMsim.

References

1. B. J. DAIR, C. C. HONEKER, D. B. ALWARD, A. AVGEROPOULOS, N. HADJICHRISTIDIS, L. J. FETTERS, M. C. CAPEL and E. L. THOMAS, *Macromolecules* Vol. 32 pp. 8145–8152 (2000).
2. A. KELLER, E. PEDEMONTE and F. M. WILLMOUTH, *Colloid and Polymer Science* **238** (1970) 385.
3. *Idem., Nature* **225** (1970) 538.
4. M. J. FOLKES, A. KELLER and F. P. SCALISI, *Colloid and Polymer Science* **251** (1973) 1.
5. J. A. ODELL and A. KELLER, *Polymer Engineering and Science* **17** (1977) 544.
6. R. G. C. ARRIDGE and M. J. FOLKES, *Journal of Physics Part D: Applied Physics* **5** (1972) 344.
7. B. J. DAIR, A. AVGEROPOULOS, N. HADJICHRISTIDIS, M. CAPEL and E. L. THOMAS, to appear in *Polymer*.
8. A. AVGEROPOULOS, B. J. DAIR, N. HADJICHRISTIDIS and E. L. THOMAS, *Macromolecules* **30** (1997) 5634.
9. R. J. ALBALAK and E. L. THOMAS, *Journal of Polymer Science Part B: Polymer Physics* **31** (1993) 37.
10. *Idem., ibid.* **32** (1994) 341.
11. J. F. NYE, *Physical Properties of Crystals* (Clarendon Press, Oxford, 1957).
12. G. E. DIETER, *Mechanical Metallurgy* (McGraw-Hill, New York, 1986).
13. F. A. MCCLINTOCK and A. S. ARGON, "Mechanical Behavior of Materials" (Addison-Wesley, Reading, MA, 1966).
14. I. M. WARD, "Mechanical Properties of Solid Polymers" (John Wiley & Sons, New York, 1975).
15. S. G. TARASOV, D. Y. TSVANKIN and Y. K. GODOVSKY, *Polymer Science USSR* **20** (1978) 1728.
16. G. HADZIIOANNOU, A. MATHIS and A. SKOULIOS, *Colloid and Polymer Science* **257** (1979) 337.
17. T. PAKULA, K. SAIJO, H. KAWAI and T. HASHIMOTO, *Macromolecules* **18** (1985) 1294.
18. C. C. HONEKER and E. L. THOMAS, *Chemistry of Materials* **8** (1996) 1702.
19. Y. COHEN, R. ALBALAK, B. J. DAIR, M. C. CAPEL and E. L. THOMAS, in preparation.
20. C. C. HONEKER, PhD., Massachusetts Institute of Technology (1997).
21. B. J. DAIR, A. AVGEROPOULOS, N. HADJICHRISTIDIS, M. CAPEL and E. L. THOMAS, in preparation.
22. *Idem.*, in preparation.
23. A. H. SCHOEN, NASA Technical Note TN D-5541 (1970).
24. K. GROSSE-BRAUCKMANN, *Journal of Colloid and Interface Science* **187** (1997) 418.
25. J. HOFFMAN, website at *http://www.msri.org/*.
26. R. J. ALBALAK, E. L. THOMAS and M. S. CAPEL, *Polymer* **38** (1997) 3819.
27. G. HOLDEN, E. T. BISHOP and N. R. LEGGE, *Journal of Polymer Science Part C* **26** (1969) 37.
28. J. F. BEECHER, L. MARKER, R. D. BRADFORD and S. L. AGGARWAL, *ibid.* **26** (1969) 117.
29. T. L. SMITH and R. A. DICKIE, *ibid.* **26** (1969) 163.
30. T. L. SMITH, in "Block Polymers," edited by S. L. Aggarwal (Plenum Press, New York, 1970) p. 137.
31. R. P. KAMBOUR, *Polymer* **5** (1964) 143.
32. R. P. KAMBOUR and A. S. HOLIK, *Journal of Polymer Science A2* **7** (1969) 1393.
33. R. P. KAMBOUR and R. R. RUSSELL, *Polymer* **12** (1971) 237.
34. P. BEAHAN, M. BEVIS and D. HULL, *Philosophical Magazine* **24** (1971) 1267.
35. B. D. LAUTERWASSER and E. J. KRAMER, *ibid.* **A 39** (1979) 469.
36. A. M. DONALD, E. J. KRAMER and R. A. BUBECK, *Journal of Polymer Science: Polymer Physics Edition* **20** (1982) 1129.
37. H. BROWN and E. J. KRAMER, *Journal of Macromolecular Science—Physics B* **19** (1981) 487.
38. A. M. DONALD and E. J. KRAMER, *Philosophical Magazine A* **43** (1981) 857.
39. A. M. DONALD, T. CHAN and E. J. KRAMER, *Journal of Materials Science* **16** (1981) 669.
40. M. FUJIMURA, T. HASHIMOTO and H. KAWAI, *Rubber Chemistry and Technology* **51** (1978) 215.
41. T. HASHIMOTO, M. FUJIMURA, K. SAIJO, H. KAWAI, J. DIAMANT and M. SHEN, in "Multiphase Polymers" edited by S. L. Cooper and G. M. Estes (ACS Advances in Chemistry Series, 1979) p. 257.
42. D. M. BRUNWIN, E. FISCHER and J. F. HENDERSON, *Journal of Polymer Science Part C* **26** (1969) 135.
43. E. FISCHER and J. F. HENDERSON, *ibid.* **26** (1969) 149.
44. G. HOLDEN and N. R. LEGGE, in "Thermoplastic Elastomers," edited by G. Holden, N. R. Legge, R. P. Quirk and H. E. Schroeder (Hanser Publishers, New York, 1996) p. 48.

Received 25 October 1999
and accepted 5 January 2000